Isothermal Crystallization Kinetics and Melting Behaviors of Nanocomposites of Poly(trimethylene terephthalate) Filled with Nano-$CaCO_3$

Mingtao Run, Chenguang Yao, Yingjin Wang, Jungang Gao

College of Chemistry and Environmental Science, Hebei University, Baoding 071002, China

Received 15 June 2006; accepted 29 June 2006
DOI 10.1002/app.24996
Published online 17 July 2007 in Wiley InterScience (www.interscience.wiley.com).

ABSTRACT: The isothermal crystallization and subsequent melting behavior of poly(trimethylene terephthalate) (PTT) composites filled with nano-$CaCO_3$ were investigated at designated temperatures with differential scanning calorimetry. The Avrami equation was used to fit the isothermal crystallization. The Avrami exponents were determined to be 2–3 for the neat PTT and PTT/$CaCO_3$ composites. The particles of nano-$CaCO_3$, acting as nucleating agents in the composites, accelerated the crystallization rate, with the half-time of crystallization decreasing or the growth rate constant (involving both nucleation and growth rate parameters) increasing. The crystallization activation energy calculated from the Arrhenius formula was reduced as the nano-$CaCO_3$ content increased from 0 to 2%, and this suggested that nano-$CaCO_3$ made the molecular chains of PTT easier to crystallize during the isothermal crystallization process. Subsequent melting scans of the isothermally crystallized composites exhibited triple or double melting endotherms: the greater the content was of nano-$CaCO_3$, the lower the temperature was of the melting peak. The degree of crystallization deduced from the melt enthalpy of composites with the proper concentration of nano-$CaCO_3$ was higher than that of pure PTT, but it was lower when the nano-$CaCO_3$ concentration was more than 2%. The transmission electron microscopy pictures suggested that the dispersion state of nano-$CaCO_3$ particles in the polymer matrix was even when its concentration was no more than 2%, whereas some agglomeration occurred when its concentration was 4%. Polarized microscopy pictures showed that much smaller or less perfect crystals formed in the composites because of the interaction between the molecular chains and nano-$CaCO_3$ particles. J Appl Polym Sci 106: 1557–1567, 2007

Key words: crystallization; composites; DSC; morphology

INTRODUCTION

Poly(trimethylene terephthalate) (PTT) is a new type of linear aromatic polyester first synthesized by Whinfield et al. in 1940,[1] but it was not commercially available then because of the high cost of 1,3-propanediol, one of the raw materials used to produce PTT. With a breakthrough in the synthesis of 1,3-propanediol at a much lower cost, PTT is now commercially available and is produced by Shell Chemicals under the trade name Corterra.[2] PTT offers several advantageous properties, including good tensile behavior, resilience, outstanding elastic recovery, and dyeability. Moreover, PTT fibers have the resiliency and softness of nylon fibers, as well as the chemical stability and stain resistance of poly(ethylene terephthalate) counterparts, and this makes them ideal candidates for applications such as carpets and other textile fibers. Hence, engineering plastics probably will be an important application field of PTT (a semicrystalline polymer).[3–6] With the industrialized production of PTT, it has received much attention from researchers.[5–10]

To extend the application fields of polymers, researchers are devoted to obtaining polymers with higher performance, and there has been much research on preparing organic/inorganic composites through the addition of inorganic particles into a polymer matrix. Inorganic particles have contributed to greatly improving crystallization, mechanical, and rheological properties.[11–16] Various inorganic particles, such as SiO_2,[17,18] TiO_2,[19,20] $CaCO_3$,[21–24] and montmorillonite, are usually used as fillers in organic/inorganic composites. The benefit of inorganic particle fillers is high rigidity with an improved yield strength or modulus, which mainly is induced by a change in the crystallization of the polymer. An adequate amount of inorganics usually promotes nucleation with an increasing crystallization rate of the polymer.[25]

$CaCO_3$ is one of the most commonly used inorganic fillers for thermoplastics, such as poly(vinyl chloride) and polypropylene;[26] however, nanoparticles less than 0.7 μm in size tend to aggregate and

Correspondence to: M. Run (rmthyp@hotmail.com).

Contract grant sponsor: Natural Science Foundation of Hebei Province; contract grant number: B2007000148.

Contract grant sponsor: Science Foundation of Hebei University; contract grant number: Y2006065.

Journal of Applied Polymer Science, Vol. 106, 1557–1567 (2007)

show very poor dispersion in composites, and agglomeration becomes worse as the particle size is reduced.[27] Therefore, there are many efforts devoted to surface-modified $CaCO_3$ particles to increase the interactions between the polymer and filler. Usually, the modifier has a long alkyl chain with one hydroxyl end group, and it is believed that the polar group is absorbed onto the surface of nanoparticles and that the long alkyl chain is compatible with polymer molecular chains.[28,29] The addition of a modifier reduces the particle/particle interaction by lowering the surface free energy of nanoparticles, and there is better dispersion of the nanoparticles in the polymer matrix. The effects of surface modifications are positive on the mechanical properties of composites.

Many articles about PTT and its blends with other polyesters have been published recently, focusing on the crystallization kinetics,[5,8,10,30–35] crystal morphology,[8,9] and melting behavior.[30,32] However, there are few published studies on improving the properties of PTT.[36] To the best of our knowledge, there is no report on the crystallization kinetics or crystal morphology of PTT/$CaCO_3$ nanocomposites.

In this study, tri(dioctylpyrophosphateoxy) titanate was used as a modifier to treat nano-$CaCO_3$ to prevent its agglomeration, and then various PTT/$CaCO_3$ nanocomposites were prepared by melt compounding with a corotating twin-screw extruder with different nano-$CaCO_3$ concentrations. As a kind of exterior impurity, nano-$CaCO_3$ can affect the crystallization behavior of PTT. In this study, the isothermal crystallization kinetics and subsequent melting behavior and spherulite morphology of PTT/$CaCO_3$ nanocomposites were investigated. Based on differential scanning calorimetry (DSC) measurements, a study of the isothermal crystallization kinetics was performed with the Avrami equation. The crystallization activation energy (ΔE) was also calculated with the Arrhenius method.

EXPERIMENTAL

Materials

PTT was provided in pellet form by Shell Chemicals (Montreal, Canada), and its intrinsic viscosity was measured to be 0.92 dL/g in a solution of phenol and tetrachloroethane (50/50 w/w) at 25°C with an Ubbelohde viscometer. $CaCO_3$ nanoparticles were supplied by Guangxi Chemical, Ltd. (Henzhou, China), with a size in the range of 50–70 nm. A nonionic modifier, tri (dioctylpyrophosphateoxy) titanate (CT-114), which had good stability under 285°C, was supplied by Jiangsu Lijin Chemical, Ltd. (Changzhou, China), and was used to treat the nano-$CaCO_3$ particles.

Composite preparation

The nano-$CaCO_3$ particles were dried in an oven at 110°C for 8 h, and then tri(dioctylpyrophosphateoxy) titanate, dissolved in ethanol (1 : 1 w/w), was added to the dried $CaCO_3$; the mixture was stirred for 10 min with a high-speed mixer, and then it was dried in an oven at 60°C for 3 h to obtain the modified nano-$CaCO_3$. PTT was dried in a vacuum oven for 4 h at 140°C to avoid moisture-induced degradation reactions. The dried PTT pellets and modified nano-$CaCO_3$ particles were mixed and melt-compounded in a ZSK 25WLE WP self-wiping (Stuttgart, Germany), corotating twin-screw extruder at a die temperature of 265°C and a screw speed of 140 rpm, and then the molten composites were quenched with cold water, cut into pellets, and dried in a vacuum oven at 140°C for 4 h before being used for DSC or polarized optical microscopy (POM) measurements. Corresponding to the weight percentage of nano-$CaCO_3$, the names of the composites were PTT (0% $CaCO_3$), PTT1 (1% $CaCO_3$), PTT2 (2% $CaCO_3$), and PTT4 (4% $CaCO_3$).

Analysis

The dispersion state of the nano-$CaCO_3$ particles in the polymer matrix was examined with a Hitachi 900 transmission electron microscope (Tokyo, Japan). Samples for POM measurements were prepared through the sandwiching of a tiny pellet of a PTT/$CaCO_3$ composite between two glass plates, compression at 260°C for 5 min, and then annealing in an oven at 210°C for 3 h. POM observations were performed with a Leitz SM-LUX-POL (Benshiem, Germany) with a camera.

The melting and crystallization behaviors of four samples were investigated with the following program: the dried samples were first heated at a heating rate of 100°C/min from room temperature to 260°C under a nitrogen atmosphere, held for 5 min and then cooled to 50°C at a cooling rate of 200°C/min to obtain amorphous-state samples, then heated again at a rate of 10°C/min to 260°C, and held there for 5 min and then cooled to 50°C at a rate of 10°C/min. The second heating and cooling processes were recorded with a PerkinElmer Diamond DSC instrument (Shelton, CT).

Isothermal crystallization and subsequent melting processes were performed as follows: the samples were heated at a rate of 100°C/min to 260°C, held there for 5 min, and then cooled to the designated crystallization temperature (T_c) rapidly (200°C/min). After the isothermal crystallization was finished, the samples were heated to 260°C at a rate of 10°C/min.

RESULTS AND DISCUSSION

Dispersion state of the nanoparticles

Transmission electron microscopy micrographs of PTT1, PTT2, and PTT4 are shown in Figure 1. For

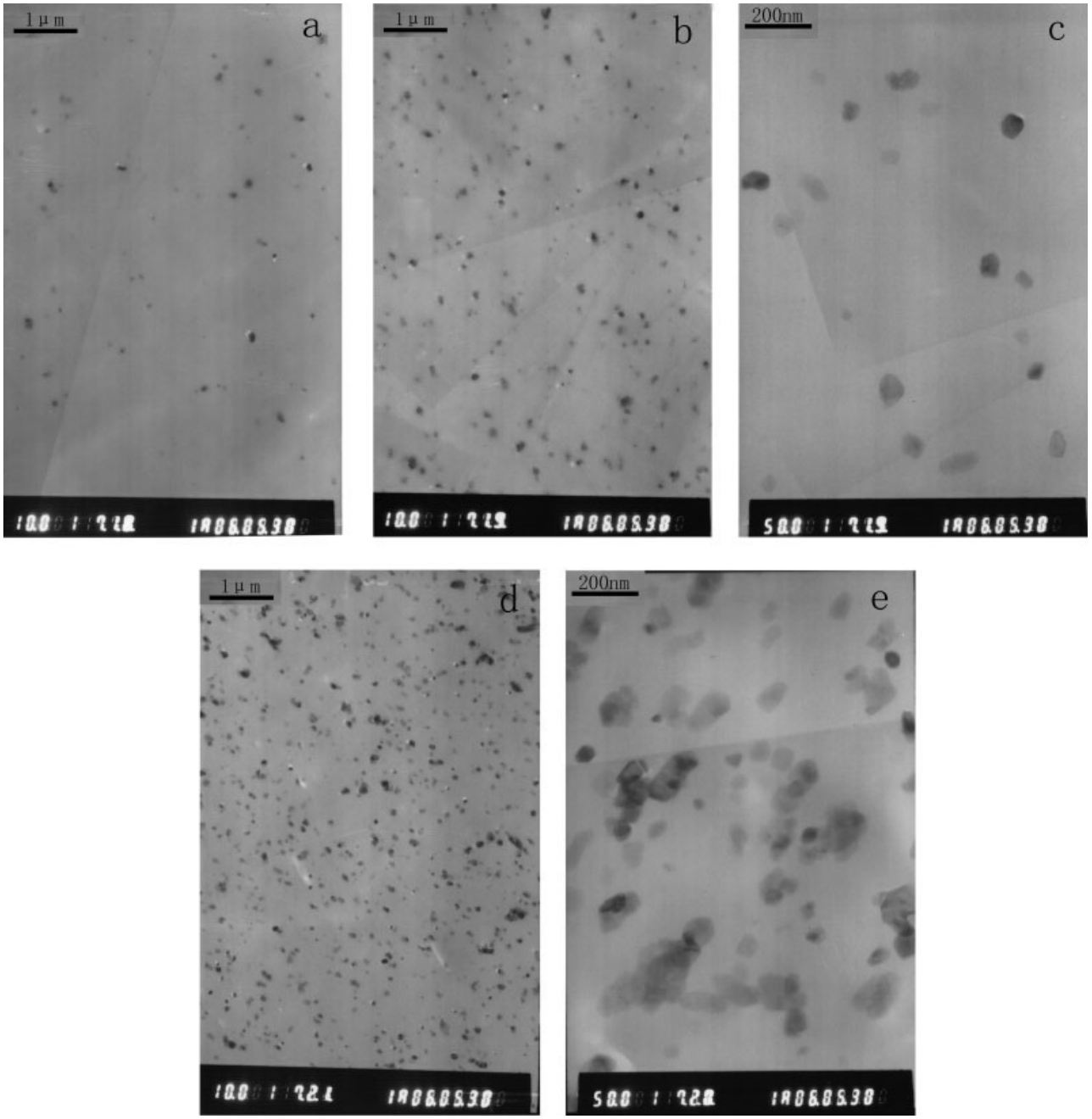

Figure 1 Transmission electron micrographs of nanocomposites with different magnifications: (a) PTT1 (10,000×), (b) PTT2 (10,000×), (c) PTT2 (50,000×), (d) PTT4 (10,000×), and (e) PTT4 (50,000×).

PTT1 [Fig. 1(a)] and PTT2 [Fig. 1(b,c)], a good dispersion state of nano-$CaCO_3$ particles in the matrix can be observed, and no agglomeration occurs; however, for PTT4 [Fig. 1(d,e)], the dispersion state of nano-$CaCO_3$ particles is not so good, and some agglomerations 200–300 nm in size can be observed, which are several times larger than the primary size of 50–70 nm. These results indicate that the shear force of melt extrusion is not enough to break down all the agglomerations, especially at relatively high filler concentrations (e.g., 4%). The agglomeration of nano-$CaCO_3$ may affect the crystallization behavior of PTT nanocomposites.

Melting and crystallization behavior

Typical melting DSC curves of the four samples are shown in Figure 2, and the kinetic parameters of the melting curves are summarized in Table I. The neat PTT exhibits an apparent glass transition at about 54°C, a cold-crystallization peak at about 87°C, and a melting peak at about 224°C. However, neither an

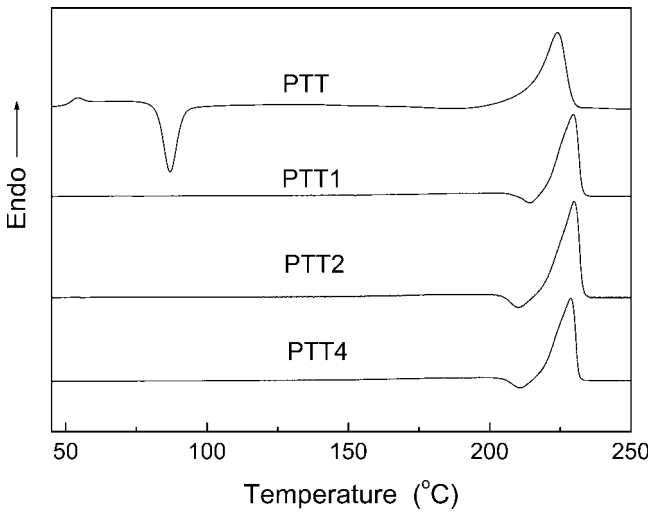

Figure 2 Second-heating DSC curves of the nanocomposites.

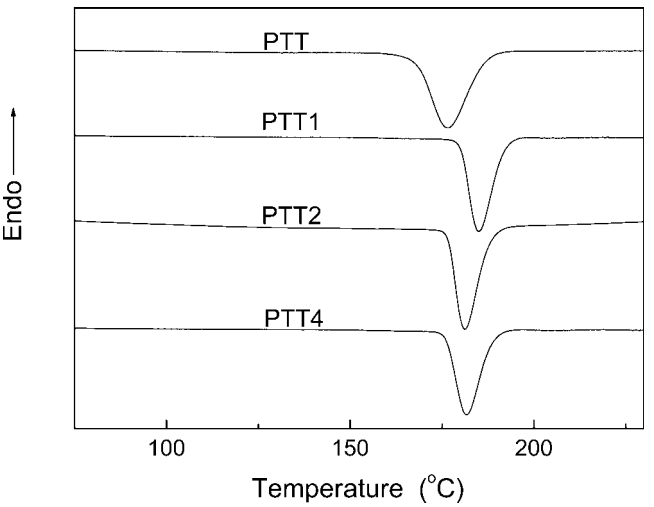

Figure 3 Melt-crystallization DSC curves of four nanocomposites.

obvious glass transition nor cold crystallization is observed for samples PTT1, PTT2, and PTT4. In the DSC curve of neat PTT, the cold-crystallization peak area is smaller than the melting peak area, and this indicates that at the cooling rate of 200°C/min, the molten PTT is frozen in the amorphous state directly, whereas the molten PTT1, PTT2, and PTT4 composites are essentially turned into semicrystalline ones at the same cooling rate. It is also recognized that the melting peaks of PTT1, PTT2, and PTT4 shift to a higher temperature in comparison with neat PTT. Moreover, an obvious recrystallization peak can be observed around 210°C in each curve of PTT1, PTT2, and PTT4, whereas no recrystallization peak is shown in the curve of neat PTT; this indicates that semicrystalline PTT1, PTT2, and PTT4 are more likely to undergo a melting/recrystallization process during DSC scanning.[37]

The melt-crystallization behaviors of four composites at the cooling rate of 10°C/min are shown in Figure 3, and the kinetic parameters of the cooling process are summarized in Table I. At this cooling rate, the crystallization exothermal peaks of PTT1, PTT2, and PTT4 are shifted to a high temperature in comparison with neat PTT, and this indicates that nano-$CaCO_3$ particles can increase the melt-crystallization temperature. However, in comparison with the temperature of the melt-crystallization peak in the cooling scans of PTT4 and PTT1, the temperature is reduced by 3.4°C, and the effects of heterogeneous nucleation decrease a little; this may be induced by the agglomeration of nano-$CaCO_3$ particles.

Isothermal crystallization kinetic analysis

Isothermal crystallization behavior

Exothermal diagrams of the isothermal crystallization analysis for PTT and PTT/$CaCO_3$ composites are shown in Figure 4(a,b). With T_c increasing, the exothermal peaks of each curve are shifted to longer times, and this indicates that T_c is an important

TABLE I
Kinetic Parameters of Melting and Crystallization for Various Samples

	Heating scan						Cooling scan	
Sample	T_g (°C)[a]	$T_{c,c}$ (°C)[b]	ΔH_c (J/g)[c]	T_{rec} (°C)[d]	T_m (°C)[e]	ΔH_m (J/g)[f]	$T_{c,h}$ (°C)[g]	ΔH (J/g)
PTT	54.0	87.0	−29.0	—	224.1	59.7	177.6	−50.5
PTT1	—	—	—	214.5	229.6	56.6	185.1	−51.4
PTT2	—	—	—	210.6	229.7	58.7	181.2	−47.2
PTT4	—	—	—	211.1	228.5	56.8	181.7	−49.6

[a] Glass-transition temperature.
[b] Temperature of the cold-crystallization peak in the heating scan.
[c] Cold-crystallization enthalpy in the heating scan.
[d] Temperature of the recrystallization peak in the heating scan.
[e] Melting temperature.
[f] Melting enthalpy.
[g] Temperature of the melt-crystallization peak in the cooling scan.

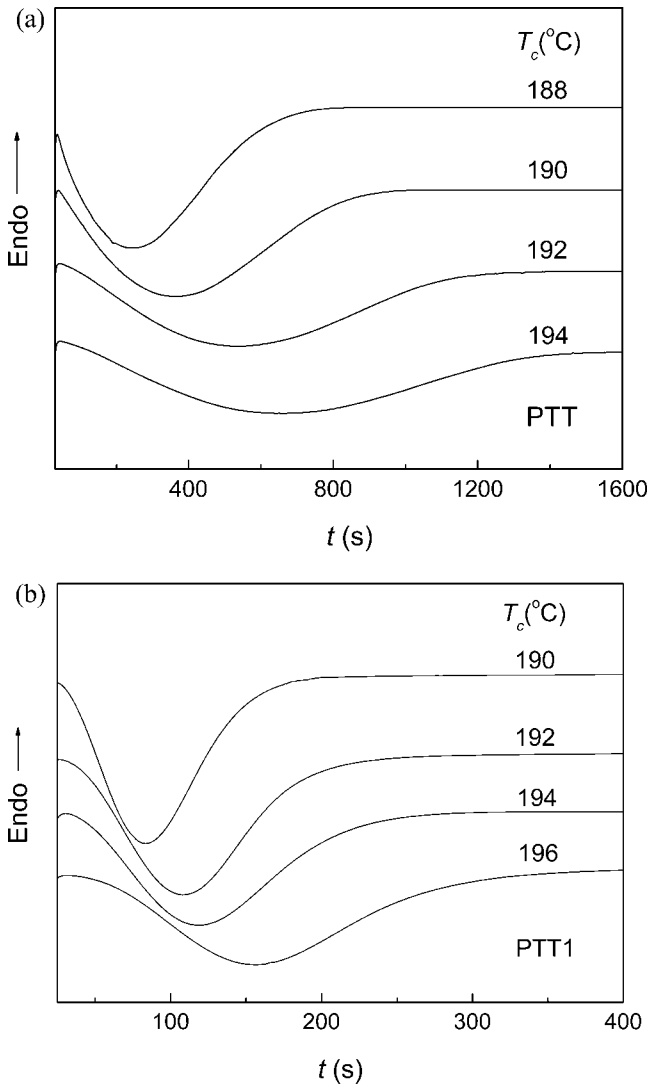

Figure 4 Heat flow versus the time during the isothermal crystallization of (a) PTT and (b) PTT1 nanocomposites at different T_c values by DSC.

influencing factor determining the crystallization time. From the data listed in Table II, the crystallization enthalpy (ΔH) of each sample increases slightly with increasing T_c, and this implies a dependence of the crystallinity on T_c; however, in a comparison of the ΔH values of PTT1, PTT2, and PTT4 with that of neat PTT, PTT1 increases but PTT2 and PTT4 decrease a little, and this indicates that the proper concentration of nano-$CaCO_3$ can improve the total crystallization, but too much can have a negative effect.

Figure 5(a,b) shows the relative crystallinity at time t [$X_c(t)$] integrated from Figure 4 as a function of the crystallization time (t) for samples PTT and PTT1 at various T_c values. In Figure 5(a,b), the characteristic sigmoidal isotherms are shifted to the right along the time axis with increasing T_c, and this indicates a progressively slower crystallization rate as T_c increases.

Another important parameter is the half-time of crystallization ($t_{1/2}$), which is defined as the time taken from the onset of $X_c(t)$ until 50% completion. The dependence of $t_{1/2}$ on T_c for various samples is shown in Figure 6 and is also listed in Table II. $t_{1/2}$ of neat PTT increases much as T_c increases from 188 to 194°C, and this indicates that neat PTT is a thermally activated crystallization polymer. PTT1, PTT2, and PTT4 show slow changes of $t_{1/2}$ with increasing T_c, and this indicates a lower dependence on T_c than that of the neat polymer. When T_c is 190°C (Table II), $t_{1/2}$ of neat PTT is evidently longer than that of PTT1, PTT2, and PTT4, and this suggests an apparent increase in the crystallization rate as nano-$CaCO_3$ particles fill into the polymer matrix. From the results, we also found that PTT4 has a larger $t_{1/2}$ value than PTT1 and PTT2; that is, the crystallization rate of PTT4 decreases compared with that of PTT1 and PTT2, and this might be caused by an agglomeration effect of nano-$CaCO_3$, as shown in Figure 1(d,e).

Analysis based on the Avrami equation

If we assume that $X_c(t)$ increases with the crystallization time (t), the Avrami equation can be used to analyze the isothermal crystallization process of the neat PTT and PTT/$CaCO_3$ composites as follows:[38,39]

$$1 - X_c(t) = \exp(-Z_t t^n) \tag{1}$$

$$\log\{-\ln[1 - X_c(t)]\} = n \log t + \log Z_t \tag{2}$$

where Avrami exponent n is a mechanism constant with a value depending on the type of nucleation and the growth dimension and Z_t is a growth rate

TABLE II
Kinetic Parameters of Isothermal Crystallization for Various Samples

Sample	T_c (°C)	n	$Z_t \times 10^{-7}$ (s^{-n})	$t_{1/2}$ (s)	ΔH (J/g)
PTT	188	2.4	170	249	−36.9
	190	2.6	57.5	355	−43.8
	192	2.5	6.9	516	−43.8
	194	2.7	3.5	626	−45.0
PTT1	190	2.5	234	64	−53.1
	192	2.6	136	87	−58.0
	194	2.5	91.2	95	−58.9
	196	2.7	17.0	133	−60.9
PTT2	188	2.4	363	58	−38.4
	190	2.4	260	69	−40.1
	192	2.5	73.0	97	−43.3
	194	2.6	31.0	130	−45.0
PTT4	188	2.3	204	68	−34.9
	190	2.5	89.1	87	−35.9
	192	2.6	36.3	111	−36.4
	194	2.8	7.08	148	−37.3

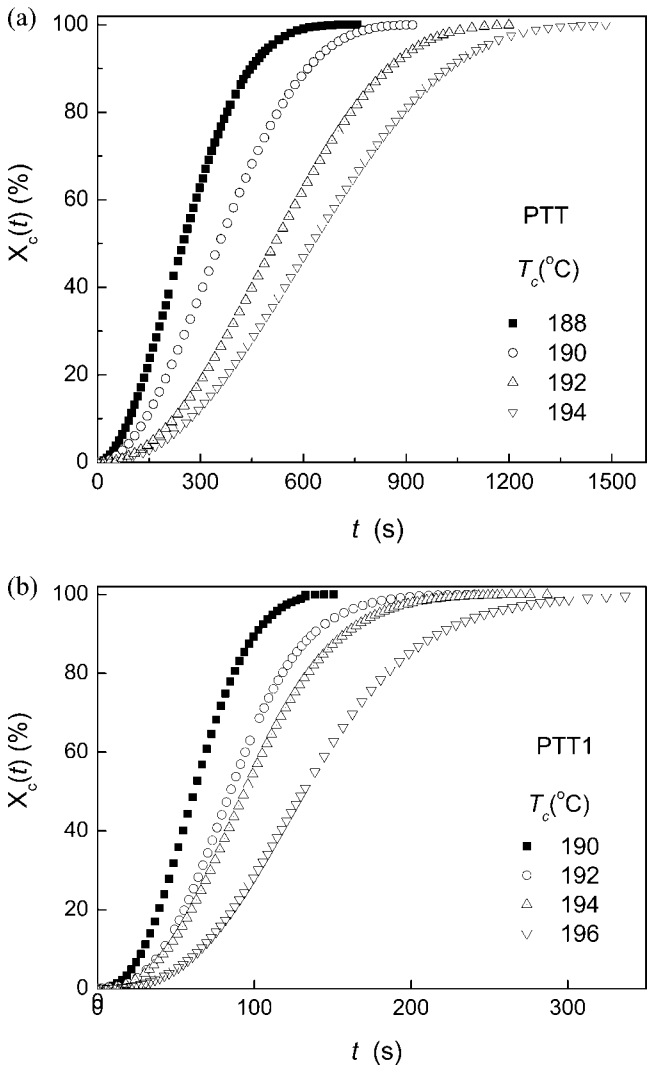

Figure 5 Development of $X_c(t)$ with t for the isothermal crystallization of (a) PTT and (b) PTT1 nanocomposites at different T_c values.

constant involving both nucleation and growth rate parameters.

The plots of $\log\{-\ln[1 - X_c(t)]\}$ versus $\log t$ according to eq. (2) are shown in Figure 7(a,b). The experimental data appear to fit very well with the Avrami equation at the primary crystallization stage, and plots of $\log\{-\ln[1 - X_c(t)]\}$ versus $\log t$ at different T_c values and nano-$CaCO_3$ concentrations are shown in a good linear relationship in the first line part.

n and Z_t can readily be extracted from the Avrami plots in Figure 7, and their values for various samples are listed in Table II. In this work, the values of n range from 2.4 to 2.7 for pure PTT in this temperature range, which, according to the definition of n,[40] may correspond to two-dimensional growth with a combination of thermal and athermal nucleation mechanisms (to pacify the fractional values of n observed). Without any heterogeneous nucleating agent, the crystal nucleus forms slowly, and the molecular chains arrange very slowly at these T_c values. As a result, crystals with a lamellar form are the predominant components of the polymer. Intuitively, the temperature dependence of n should be such that n increases with increasing T_c within the nucleation control region. This is because the number of athermal nuclei increases tremendously with decreasing T_c,[41,42] and this causes the nucleation mechanism to be more instantaneous in time and decreases the values of n.

The values of n for PTT1, PTT2, and PTT4 are about 2.6 ± 0.1, 2.5 ± 0.1, and 2.6 ± 0.2, respectively. These may be average values of various nucleation types and growth dimensions occurring simultaneously in a crystallization process in this temperature range. For PTT1, PTT2, and PTT4 with nano-$CaCO_3$ as a heterogeneous nucleus, the nucleation type should mostly be heterogeneous nucleation, and its growth dimension should mostly be a three-dimensional space extension. As a result, crystals with a spherical form are the predominant components in PTT composites.

As shown in Table II, another overall rate parameter (Z_t), which determines both the nucleating and growth processes, is extremely sensitive to temperature for each sample; that is, the higher the temperature is, the lower the crystallization rate is. Comparing the Z_t values of PTT, PTT1, PTT2, and PTT4 at the same T_c (e.g., 190°C), we find that Z_t of PTT1 and PTT2 increases sharply versus that of neat PTT, but Z_t of PTT4 is much lower than that of PTT1 and PTT2. These facts indicate that with the proper concentration of nano-$CaCO_3$ nucleating agents in a composite, the crystallization rate will be greatly increased; however, too much nano-$CaCO_3$ will reduce the crystallization

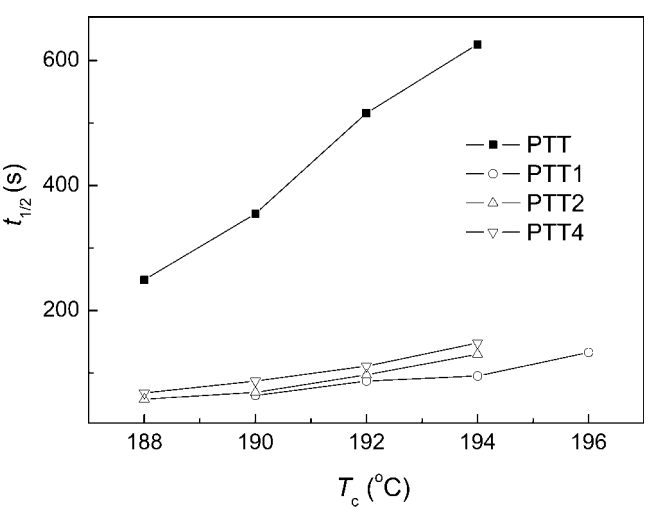

Figure 6 Plot of $t_{1/2}$ versus T_c for the isothermal crystallization of various PTT/$CaCO_3$ nanocomposites.

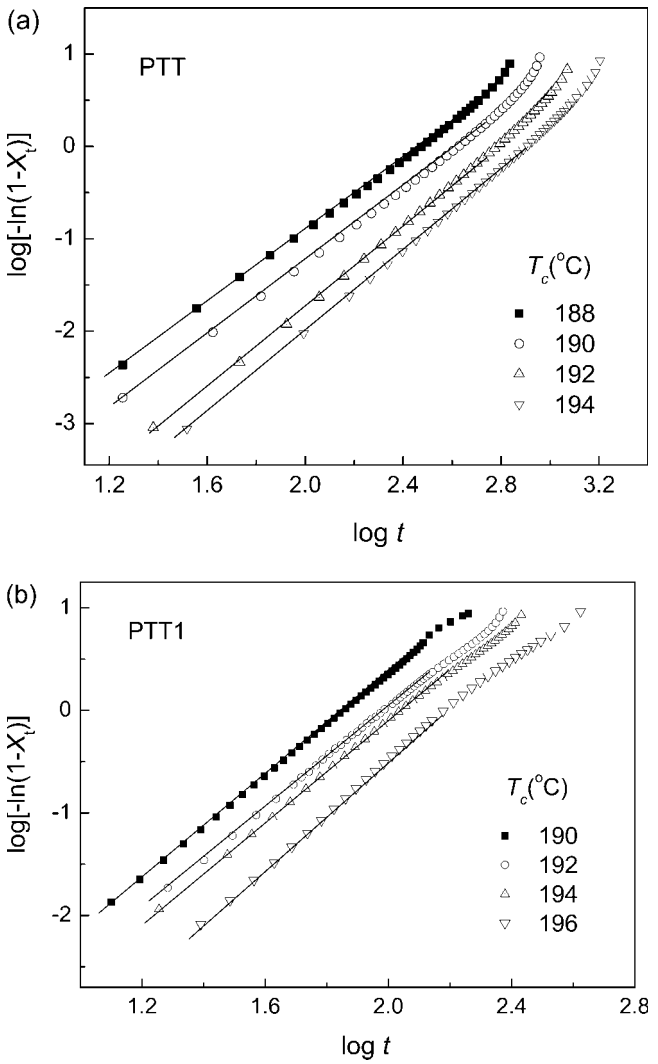

Figure 7 Plots of $\log\{-\ln[1 - X_c(t)]\}$ versus $\log t$ for (a) PTT and (b) PTT1 nanocomposites at the indicated temperatures.

rate. There are probably two reasons. First, although the nanoparticles are surface-treated with tri(dioctylpyrophosphateoxy) titanate, the dispersion state in the PTT matrix may not be as even as expected, as shown in Figure 1(d,e), and agglomeration phenomena will occur, especially at high particle concentrations; second, the number of nanoparticles is so large that only a small fraction of them serve as nuclei, whereas most particles may cause an increase in the melt viscosity, resulting in the restriction of molecular movement into an orderly packing state.

Subsequent melting behaviors

The triple melting phenomenon of PTT has previously been reported.[30–32,34,37] The occurrence of peak I at a lower temperature has been attributed to recrystallization during the reheating process, and peaks II and III at higher temperatures have been attributed to the melting of the primary crystallites of two populations of lamellar stacks.[30] In a separate investigation about multiple melting behavior in isothermally crystallized PTT using DSC and wide-angle X-ray diffraction techniques,[31] it was observed that the subsequent melting thermograms for PTT isothermally crystallized within the T_c range of 182–215°C exhibited a triple (for T_c values lower than ca. 192°C), double (for T_c values greater than ca. 192°C but lower than ca. 210°C), or single (for T_c values greater than ca. 210°C) endothermic melting phenomenon. For the triple melting phenomenon, it was postulated that the occurrence of peak I was a result of the melting of the primary crystallites formed at T_c, peak II was a result of the melting of recrystallized crystallites that formed during a heating scan, and peak III was a result of the melting of recrystallized crystallites of different stabilities that formed during a heating scan.

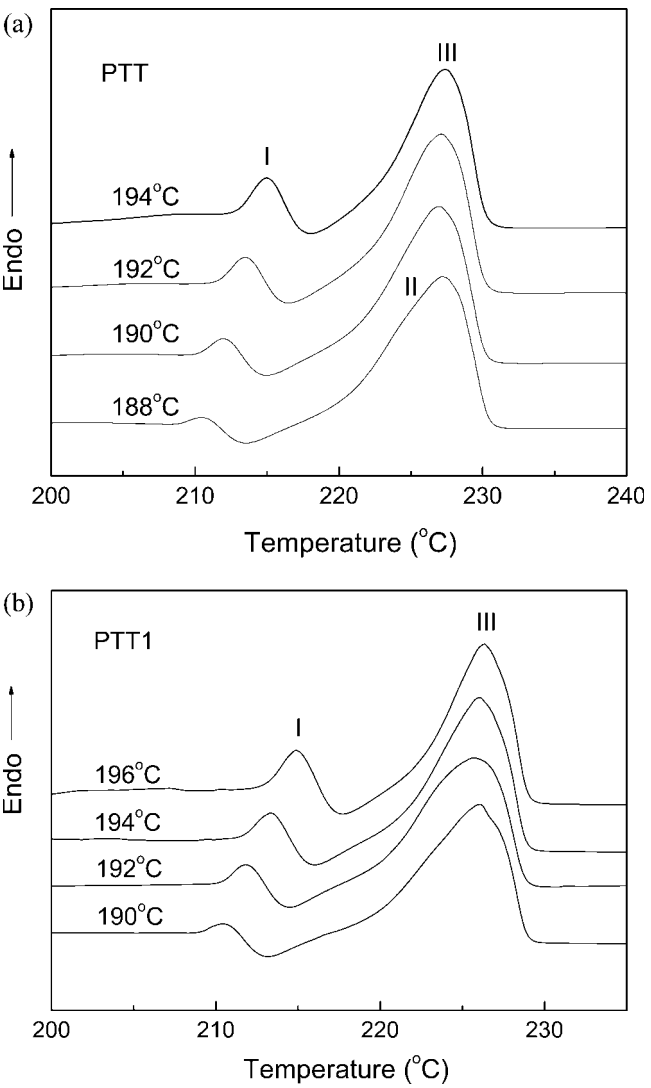

Figure 8 Melting endotherms of (a) PTT and (b) PTT1 nanocomposites recorded at a heating rate of 10°C/min after isothermal crystallization at the specified temperatures.

TABLE III
Melting Endotherm Parameters of Various Samples

Sample	T_c (°C)	T_{mI} (°C)[a]	ΔH_{fI} (J/g)[b]	T_{mII}[c] (°C)	T_{mIII}[d] (°C)	$\Delta H_{fII+III}$ (J/g)[e]	T_{rec} (°C)[f]
PTT	188	210.4	0.46	225.3	227.2	44.6	213.6
	190	212.3	1.44	—	227.0	41.9	214.9
	192	213.5	2.36	—	227.2	37.8	216.5
	194	215.0	3.53	—	227.3	34.3	218.0
PTT1	190	210.5	0.87	—	226.1	53.4	213.2
	192	211.8	1.52	—	225.7	47.6	214.5
	194	213.3	2.96	—	226.1	51.0	216.0
	196	214.8	5.00	—	226.3	46.2	217.7
PTT2	188	210.3	0.27	225.0	227.5	48.2	213.1
	190	211.6	0.66	—	227.1	44.9	214.3
	192	212.9	1.43	—	226.9	40.8	215.7
	194	214.2	2.45	—	227.0	38.3	217.1
PTT4	188	210.0	0.22	224.3	226.3	36.4	213.0
	190	211.5	0.63	—	226.5	33.1	214.4
	192	212.8	1.15	—	226.6	30.3	215.7
	194	214.2	2.00	—	226.9	30.0	217.3

[a] Melting temperature of the Peak I.
[b] Melting enthalpy of Peak I.
[c] Melting temperature of the Peak II.
[d] Melting temperature of the Peak III.
[e] Melting enthalpy of Peak II and Peak III.
[f] Temperature of the recrystallization peak in the heating scan.

Figure 8(a,b) presents DSC heating thermograms of neat PTT and PTT/$CaCO_3$ composites annealed at different T_c values, and the melting parameters are summarized in Table III. From Figure 8(a) and Table III, it is apparent that the neat PTT endotherms exhibit three melting peaks at a lower T_c value (188°C), but they show only two melting peaks when T_c is higher than 190°C because peak II and peak III tend to combine. Moreover, peaks I and II shift to higher temperatures as T_c increases from 188 to 194°C, but peak III changes little. As shown in Figure 8(a), the area of peak III is larger than that of either peak I or II, and this indicates that the major crystallization of PTT is predominantly composed of primary crystals.

Each of the melting endotherms of PTT1, PTT2, and PTT4 exhibits only two primary melting peaks: peaks I and III [e.g., the endotherms of PTT1 in Fig. 8(b)]. According to a comparison of the melting endotherms of neat PTT with those of PTT1, PTT2, and PTT4 at the same T_c (e.g., 190°C), the temperatures of peak I vary with various nano-$CaCO_3$ concentrations, and their values are 212.3 (PTT), 210.5 (PTT1), 211.6 (PTT2), and 211.5°C (PTT4), respectively. Therefore, it might be concluded that nano-$CaCO_3$ particles can increase the formation of crystallites with a smaller or poor morphology.

According to Figure 8(a,b) and Table III, a recrystallization exotherm can be observed during DSC heating, and it tends to shift to a higher temperature as T_c increases. A comparison of the recrystallization peak locations of the four samples at the same T_c (e.g., 190°C) shows that those of PTT1, PTT2, and PTT4 are all lower than that of neat PTT, and this indicates that the crystallites of PTT1, PTT2, and PTT4 are smaller or less prefect and more likely to undergo a melting/recrystallization process during a heating scan. According to the values of $\Delta H_{fII+III}$ in Table III, the crystallinity is highest when the $CaCO_3$ concentration is 1 wt % at the same T_c (e.g., 190°C), and this indicates that the degree of crystallization of the composites is dependent

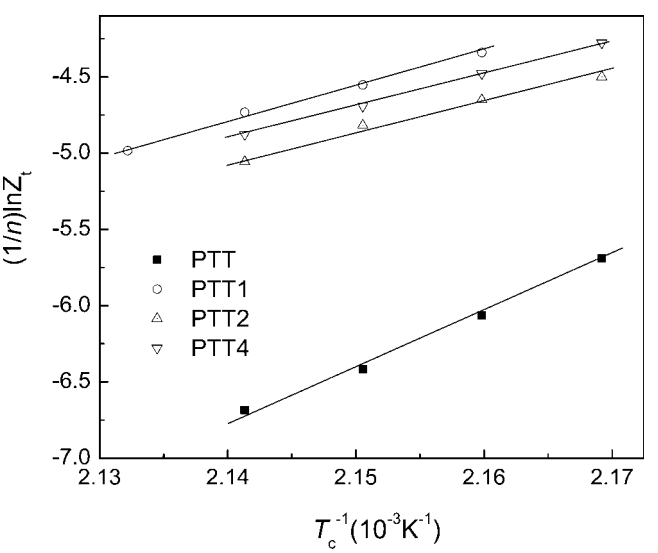

Figure 9 Plot of $(1/n)(\ln Z_t)$ versus $1/T_c$ for the different nanocomposites.

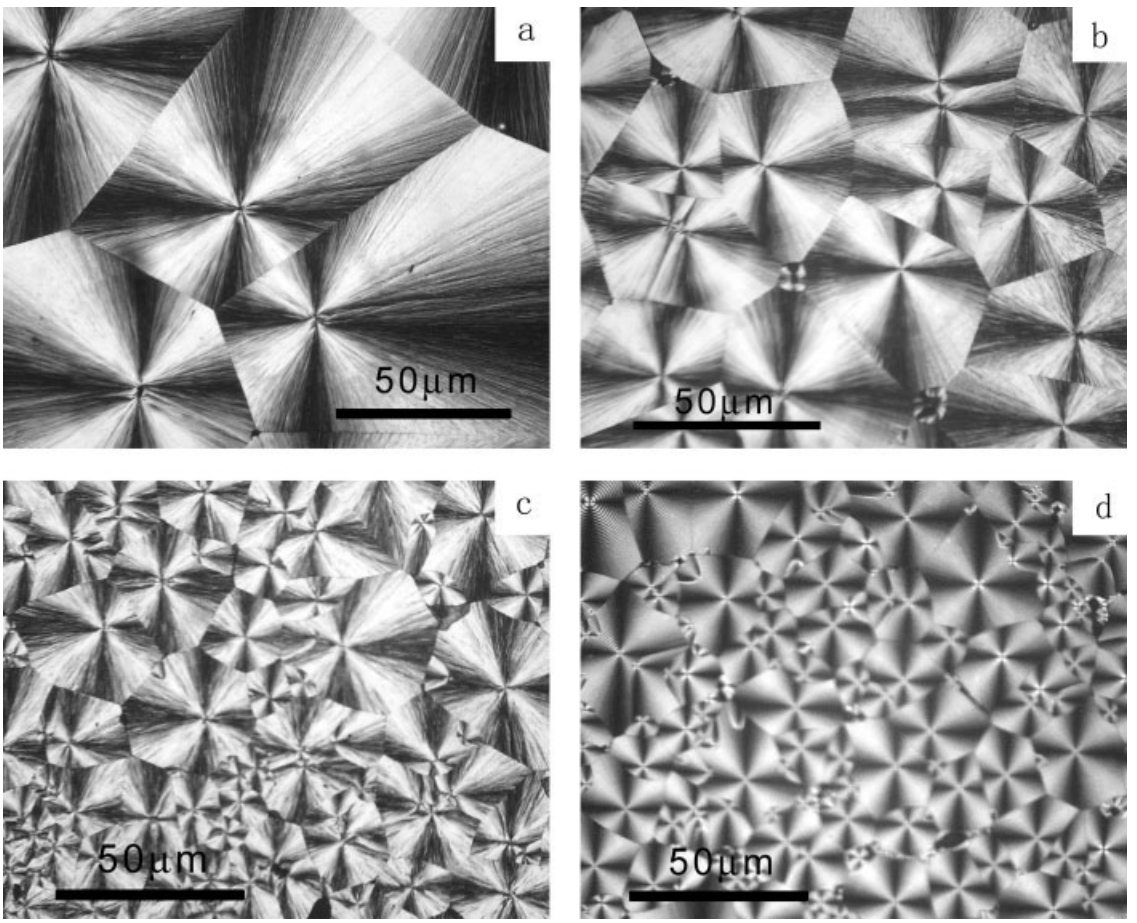

Figure 10 Polarized microscopy pictures of crystallized nanocomposites: (a) PTT, (b) PTT1, (c) PTT2, and (d) PTT4.

on the concentration of nano-$CaCO_3$, and too many nanoparticles will reduce the formation of the crystals.

ΔE

The crystallization process of neat PTT and PTT/$CaCO_3$ composites is assumed to be thermally activated. Crystallization rate parameter Z_t can be approximately described by the following Arrhenius equation:[43]

$$Z_t^{1/n} = Z_0 \exp\left(\frac{-\Delta E}{RT_c}\right) \tag{3}$$

$$\left(\frac{1}{n}\right) \ln Z_t = \ln Z_0 - \frac{\Delta E}{RT_c} \tag{4}$$

where Z_0 is the temperature-independent pre-exponential factor and R is the gas constant. ΔE can be determined by the slope coefficient of plots of $(1/n)$ ln Z_t versus $1/T_c$ [eq. (4)], which are shown in Figure 9. Because it has to release energy when the molten fluid is transformed into the crystalline state, the value of ΔE is negative on the basis of the concept of the heat quantity in physical chemistry. In this study, the ΔE values for various samples in the primary crystallization stage are −298.8 (PTT), −190.3 (PTT1), −164.5 (PTT2), and −180.4 kJ/mol (PTT4). This result suggests that ΔE of the composites decreases as the nano-$CaCO_3$ concentration increases to 2%, indicating that the proper concentration of nanoparticles acting as nucleating agents in the polymer matrix will improve the nucleation rate and induce the arrangement of molecular chains on the surface of nano-$CaCO_3$; however, too many nanoparticles (e.g., 4%) will increase ΔE and constrain the arrangement of molecular chains, probably because of an agglomeration effect. This result is also confirmed by the conclusion of a relationship between Z_t, $t_{1/2}$, and the nanoparticle concentration in the polymer matrix, as mentioned previously.

An increase in the crystallization rate and a reduction of ΔE are common characteristics for polymer/nanoparticle composites.[27] In addition to the function of tri(dioctylpyrophosphateoxy) titanate in lowering the surface free energy of nano-$CaCO_3$, the polymer/particle adhesion is also lowered by the modifier, and this results in a reduction of the constraint effect of the nano-$CaCO_3$ particles on the PTT

molecular chains. Part of the modifier also acts as a plasticizer for PTT, increasing the free volume of PTT. Therefore, the activation energy for the transport of PTT molecular segments to the crystallization front is reduced, and this leads to an increasing spherulite growth rate when the modifier is used.

Crystal morphology

After 3 h of annealing at 210°C, the crystal morphology of PTT, PTT1, PTT2, and PTT4 was observed with polarized microscopy, and four pictures are shown in Figure 10. For neat PTT, several spherulites, impinging against one another, are fairly big and perfectly grown, with a Maltese cross clearly observed with a diameter greater than 100 μm, and the interfaces between the spherulites are sharp and clear. However, the PTT1, PTT2, and PTT4 composites have relatively small or less perfect Maltese crosses, and their dimensions are reduced to 50, 30, and 20 μm or less, respectively. Clearly, the dimensions of the spherulites decrease with an increasing number of nanoparticles in the PTT matrix. These results may indicate that nano-$CaCO_3$ particles in the composites act as seeds for spherulite growth and that the crystals may grow on the surface of the nano-$CaCO_3$ particles. As the spherulites grow, they may be confined by one another and the nano-$CaCO_3$ particles as well, and this leads to more spherulites forming in a limited space. Therefore, with an increasing concentration of nanoparticles in the PTT matrix, the dimensions of the spherulites decrease gradually.

CONCLUSIONS

PTT/$CaCO_3$ nanocomposites prepared by melt compounding have been investigated with respect to the isothermal crystallization kinetics and crystal morphology. The dispersion state of nano-$CaCO_3$ particles in the polymer matrix is even when the concentration is no more than 2%, whereas some agglomeration is observed when the concentration is 4%. n and Z_t, calculated with the Avrami equation, indicate that the nanoparticles, acting as nucleating agents, accelerate the nanocomposite crystallization rate. ΔE is reduced as the nano-$CaCO_3$ concentration increases from 0 to 2%, and the nanoparticles make PTT easier to crystallize during the isothermal crystallization process; however, too high a nanoparticle concentration (e.g., 4%) will reduce the crystallization ability of the PTT matrix. Moreover, the proper concentration of nano-$CaCO_3$ particles (1%) leads to the maximum improvement in the crystallinity and crystallization rate. However, the positive influence is not increased with an increasing concentration of nanoparticles when it is more than 2%, and this may be the reason for agglomerated nano-$CaCO_3$; therefore, nano-$CaCO_3$ may be a good nucleating agent for PTT if agglomeration can be avoided. The observation of subsequent melting endotherms of neat PTT and PTT/$CaCO_3$ composites after isothermal crystallization at the specified T_c values shows double or triple melting peaks. The nano-$CaCO_3$ particles can increase the formation of microcrystallites with a smaller or poor morphology. POM observations also confirm that nanocomposites form much smaller, uniform spherulites than neat PTT, and the dimensions of the crystal decrease greatly with an increasing concentration of nanoparticles.

References

1. (a) Whinfield, J. R.; Dickson, J. T. Br. Pat. 578,079 (1941); (b) Whinfield, J. R.; Dickson, J. T. U.S. Pat. 2,465,319 (1949).
2. Chuah, H. H. Chem Fibers Int 1996, 46, 424.
3. Ward, I. M.; Wilding, M. A. Polymer 1977, 18, 327.
4. Desborough, I. J.; Hall, I. H.; Neisser, J. Z. Polymer 1979, 20, 545.
5. Huang, J. M.; Chang, F. C. J Polym Sci Part B: Polym Phys 2000, 38, 934.
6. Liu, Z. J.; Chen, K. Q.; Yan, D. Y. Eur Polym J 2003, 39, 2359.
7. Chisholm, B. J.; Zimmer, J. G. J Appl Polym Sci 2000, 76, 1296.
8. Ho, R. M.; Ke, K. Z.; Chen, M. Macromolecules 2000, 33, 7529.
9. Wang, B. J.; Li, C. H.; Hanzlicek, J.; Cheng, S. Z. D.; Geil, P. H.; Grebowicz, J.; Ho, R. M. Polymer 2001, 42, 7171.
10. Pyda, M.; Wunderlich, B. J Polym Sci Part B: Polym Phys 2000, 38, 622.
11. Fann, D. M.; Huang, S. K.; Lee, J. J Polym Eng Sci 1988, 38, 265.
12. Evstatiev, M.; Fakirov, S. Polymer 1992, 33, 877.
13. Xu, W.; Ge, M.; He, P. J Appl Polym Sci 2001, 82, 2281.
14. Yang, H.; Cao, J.; Ao, W.; Qiu, G. Polym Mater Sci Eng 2003, 19, 68.
15. Arkhireeva, A.; Hay, J. N. Polym Polym Compos 2004, 12, 101.
16. Chang, J.; Kim, S. J.; Joo, Y. L.; Im, S. Polymer 2004, 45, 919.
17. Run, M. T.; Wu, S. Z.; Zhang, D. Y.; Wu, G. Polymer 2005, 46, 5308.
18. Petrovicova, R.; Knight, R.; Schadler, L. S.; Twadowski, T. E. J Appl Polym Sci 2000, 78, 2272.
19. Petrovic, Z. S.; Javni, I.; Waddon, A.; Banhegi, G. J Appl Polym Sci 2000, 76, 133.
20. Gao, X.; Mao, L. X.; Li, N.; Jin, R. G. China Plast 2003, 17, 36.
21. Gao, X.; Mao, L. X.; Li, N.; Li, J. Eng Plast Appl 2003, 31, 2.
22. Rong, M. Z.; Zhang, M. Q.; Zheng, Y. X.; Zeng, H. M.; Walter, R.; Friedrich, K. Polymer 2001, 42, 167.
23. Rong, M. Z.; Zhang, M. Q.; Zheng, Y. X.; Zeng, H. M.; Friedrich, K. Polymer 2001, 42, 3301.
24. Hasegawa, N.; Okamoto, H.; Kato, M.; Usaki, A. J Appl Polym Sci 2000, 78, 1918.
25. Levita, G.; Marchetti, A.; Lazzeri, A. Polym Eng Sci 1989, 19, 39.
26. Chan, C. M.; Wu, J. S.; Li, J. X.; Cheung, Y. K. Polymer 2002, 43, 2981.
27. Zhang, Q. X.; Yu, Z. Z.; Xie, X. L.; Mai, Y. W. Polymer 2004, 45, 5985.
28. Akoval, G.; Akman, M. A. Polym Int 1997, 42, 195.
29. Khunova, V.; Hurst, J.; Janigova, I.; Smatko, V. Polym Test 1999, 18, 501.
30. Chung, W. T.; Yeh, W. J.; Hong, P. D. J Appl Polym Sci 2002, 83, 2426.

31. Srimoaon, P.; Dangseeyun, N.; Supaphol, P. Eur Polym J 2004, 40, 599.
32. Dangseeyun, N.; Srimoaon, P.; Supaphol, P.; Nithitanakul, M. Thermochim Acta 2004, 409, 63.
33. Hong, P. D.; Chung, W. T.; Hsu, C. F. Polymer 2002, 43, 3335.
34. Apiwanthanakorn, N.; Supaphol, P.; Nithitanakul, M. Polym Test 2004, 23, 817.
35. Xue, M. L.; Sheng, J.; Yu, Y. L.; Chuah, H. H. Eur Polym J 2004, 40, 811.
36. Tsumashima, K.; Suzuki, M. Jpn. Pat. 08,104,763 (1996).
37. Wu, P. L.; Woo, E. M. J Polym Sci Part B: Polym Phys 2003, 41, 80.
38. Avrami, M. J Chem Phys 1940, 8, 212.
39. Avrami, M. J Chem Phys 1939, 7, 1103.
40. Wunderlich, B. Macromolecular Physics; Academic: New York, 1976; Vol. 2, p 132.
41. Supaphol, P.; Spruiell, J. E. J Appl Polym Sci 2000, 75, 337.
42. Janeschitz-Kriegl, H.; Ratajski, E.; Wippel, H. Colloid Polym Sci 1999, 277, 217.
43. Cebe, P.; Hong, S. D. Polymer 1986, 27, 1183.